THE JOURNAL OF PHYSICAL CHEMISTRY A

Article

pubs.acs.org/JPCA

Effect of Strong Electric Field on the Conformational Integrity of Insulin

Xianwei Wang,[†] Yongxiu Li,[†] Xiao He,*[,†,‡] Shude Chen,[†] and John Z. H. Zhang*[,†,‡]

[†]State Key Laboratory of Precision Spectroscopy, Department of Physics, Institute of Theoretical and Computational Science, East China Normal University, Shanghai 200062, China

[‡]NYU-ECNU Center for Computational Chemistry at NYU Shanghai, Shanghai 200062, China

Supporting Information

ABSTRACT: A series of molecular dynamics (MD) simulations up to 1 μs for bovine insulin monomer in different external electric fields were carried out to study the effect of external electric field on conformational integrity of insulin. Our results show that the secondary structure of insulin is kept intact under the external electric field strength below 0.15 V/nm, but disruption of secondary structure is observed at 0.25 V/nm or higher electric field strength. Although the starting time of secondary structure disruption of insulin is not clearly correlated with the strength of the external electric field ranging between 0.15 and 0.60 V/nm, long time MD simulations demonstrate that the cumulative effect of exposure time under the electric field is a major cause for the damage of insulin's secondary structure. In addition, the strength of the external electric field has a significant impact on the lifetime of hydrogen bonds when it is higher than 0.60 V/nm. The fast evolution of some hydrogen bonds of bovine insulin in the presence of the 1.0 V/nm electric field shows that different microwaves could either speed up protein folding or destroy the secondary structure of globular proteins deponding on the intensity of the external electric field.

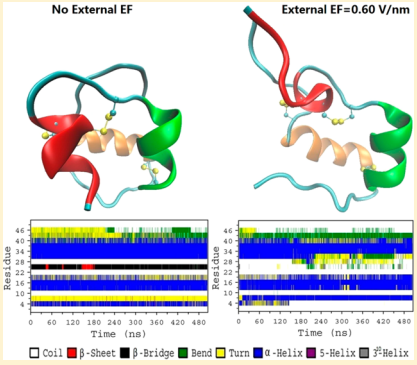

1. INTRODUCTION

The maintenance of correct conformation of a protein is critical to its function. The thermodynamic equilibrium of protein could shift to its denatured state under strong exogenous stimulations.[1−8] Several theoretical and experimental works have been carried out to detect the effect of the exogenous perturbation on protein folding and unfolding processes such as temperature,[9−12] pressure,[11−13] pH changes,[14] and laser excitation.[15] Currently, an active research field is to study the effect of external electric fields acting on proteins.[1,3,5,7,8,11,16−31] It has been experimentally confirmed that microwave radiation could alter protein conformation without bulk heating.[1] The fact that the change of protein conformation can alter the function of protein has been verified by theoretical[7,24] and experimental[1] works using amyloid, whose formation of fibrils would result in diseases such as Alzheimer's disease, cystic fibrosis, and variant Creutzfeldt−Jakob disease. The rates of protein folding and unfolding in solution could be accelerated under the microwave conditions, which is also reported and demonstrated experimentally.[3] Despite extensive experimental literatures on the study of nonthermal effects on the protein structure and function in far-infrared and microwave fields, it is still difficult for traditional experimental approaches to provide the details of these processes at the atomic level.

In recent years, computer simulation has emerged as a powerful tool to study dynamical processes of proteins in nanoseconds or microseconds and even longer time at the atomic level.[32−34] Therefore, many studies have successfully explained the observed spectral data,[35−39] revealed the chemical reaction mechanism[40−44] and given a more detailed interpretation for dynamic behavior of peptides or proteins in an external electric field[4,6,8,10,16,24,25,27] with the help of molecular dynamics (MD) simulations.

Previous MD simulations have given evidence that the protein could be denatured in several nanoseconds under the action of a strong external electric field.[4−8,16,18,24,25] Most MD simulations have demonstrated that the external electric field should be greater than 0.5 V/nm to cause damages on the secondary structure and disrupt the hydrogen bonds in proteins, whereas an external electric field of 0.1 V/nm has a significant impact on the dynamical behavior of proteins.[4−8,16,18,25] Budi and co-workers[4,16,18] performed MD simulations on the insulin chain-B in both static and oscillating external electric fields and predicted that specific frequencies of oscillating external electric fields have more destabilizing effect on the protein than the static electric field with the same strength. A similar phenomenon has also been observed in MD simulations of chignolin,[6,45] a typical β-hairpin peptide. As a result of the deficiency of flexibility for proteins under a strong

Special Issue: International Conference on Theoretical and High Performance Computational Chemistry Symposium

Received: January 29, 2014
Revised: May 3, 2014

   dx.doi.org/10.1021/jp501051r | J. Phys. Chem. A XXXX, XXX, XXX−XXX

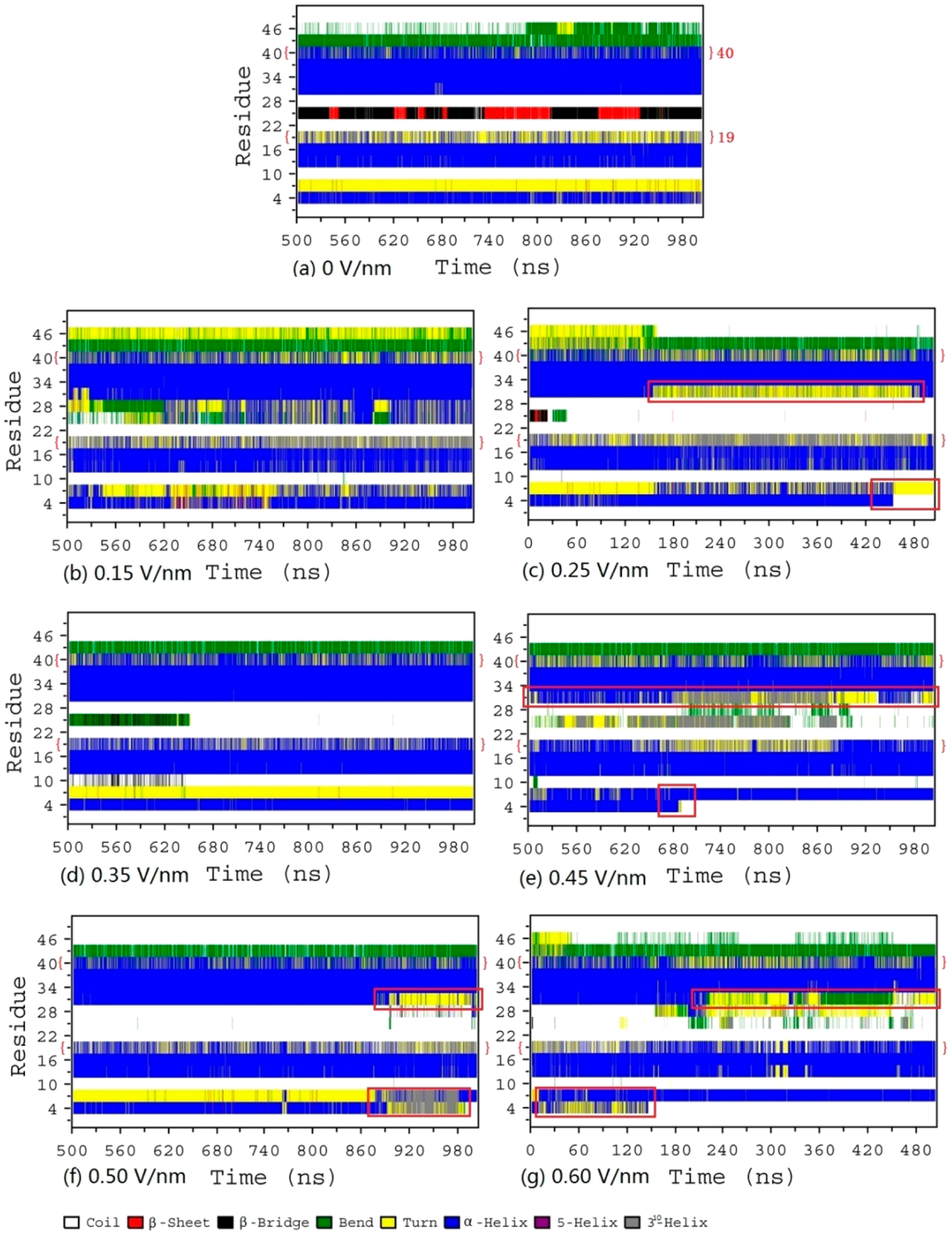

Figure 1. Evolution of the secondary structure of the bovine insulin as a function of MD simulation time in the absence of an external electric field (a) and in the presence of external electric fields of 0.15 (b), 0.25 (c), 0.35 (d), 0.45 (e), 0.50 (f), and 0.60 V/nm (g), respectively.

exogenous stimulation, their biological activity could be seriously affected.

Most MD simulation studies focused on the study of dynamical behaviors of proteins under external electric fields ranging from 10 to 100 ns time scale. This time scale is likely too short to observe disruption of protein's secondary structure, which may only be observed after a sufficiently long time MD simulation. In this study, we investigate the effect of an external electric field on the integrity of the secondary structure of insulin with relatively long MD simulations of up to 1 μs. In this work, we choose bovine insulin, which was used in the treatment of diabetes by injection as a model system. Bovine insulin differs from human insulin with only three residues in the amino acid sequence and has a three-dimensional structure similar to that of human insulin, thus having physiological effects similar to those of its human counterpart. Because of its biological significance in promoting growth and regulating blood sugar levels, insulin has been studied by many experimental and theoretical researchers.[1,4,16,18] Although the insulin is produced and stored as a hexamer in the body, it

dx.doi.org/10.1021/jp501051r | J. Phys. Chem. A XXXX, XXX, XXX−XXX

exercises its biological activity in the form of a monomer. Hence, the monomer of bovine insulin was chosen as the model system in MD simulations.

In this study, we applied static electric fields with different strengths ranging from 0.15 to 1.0 V/nm to act on the bovine insulin. Our main goal is to investigate the effect of external electric fields on protein's secondary structure with relatively long MD simulations of up to 1 μs. Our work also aims to understand the underlying mechanism of the disruption of the intraprotein hydrogen bond under external electric fields, by virtue of which we aim to elucidate the origin of denaturation of protein secondary structures under strong external electric fields at the atomistic level.

2. COMPUTATIONAL APPROACH

All MD simulations were performed using the GROMACS package v4.5.4.[46] The Amber03 force field[47] and TIP3P[48] water model were adopted for the protein and solvents, respectively. The uniform external electric field $\mathbf{E}_{ext}$ acts directly on the point charges of protein. Therefore, the modified equation of motion is given by

$$m_i\ddot{\mathbf{r}}_i = \mathbf{f}_i = \frac{\partial}{\partial r_i}U + q_i\mathbf{E}_{ext} \quad (1)$$

where $\mathbf{f}_i$ is the force on atom i of the protein when the external electric field was applied, U is the intramolecular potential, and q_i is the charge of atom i.

The starting geometry of bovine insulin was taken from the Protein Data Bank (PDB accession code 2A3G).[49] This protein is composed of 51 amino acids with chain-A (21 amino acid residues) and chain-B (30 amino acid residues). The two chains are linked together by two disulfide bonds between residues A7-B7 and residues A20-B19. Another disulfide bond is between residues A6 and A11. The first monomer was selected from the X-ray structure. The amine groups were fully protonated (Lys, Arg residues, and N-terminal), and the carboxylic groups were deprotonated (Asp, Glu residues, and C-terminal). All His residues were left neutral and protonated at the ND1 or NE2 position base on the local electrostatic environment. The protein was placed in an octahedral box whose surface to the closest atom of the solute was set to 10 Å. Subsequently, 3836 water molecules were filled in the box and two sodium ions were added for neutralizing the entire system.

The system was first energy minimized using the steepest descent algorithm for 50 000 steps to remove close contacts. Then, two 100 ps equilibrations were carried out in the constant temperature, constant volume (*NVT*) ensemble and in the constant temperature, constant pressure (*NPT*) ensemble, successively. Before the external electric field is switched on, a pre-equilibrium MD simulation was run for 60 ns at 300 K using the Berendsen thermostat[50] with a time constant of 0.1 ps. The pressure was maintained at 1 atm using the Parrinello–Rahman barostat[51] with a time constant of 2.0 ps. A time step of 2 fs was chosen for all the MD simulations. All bond lengths were constrained using LINCS algorithm.[52] Particle mesh Ewald[53] summation was employed to account for long-range electrostatics and a 10 Å cutoff for the van der Waals interaction was implemented. DSSP program[54] was utilized to calculate the time evolution of the secondary structure along the MD trajectory. Other data were analyzed by GROMACS or in-house programs. VMD software[55] was utilized to draw structural diagrams.

Several production runs of 1 μs MD simulation were performed in the presence of static external electric fields with intensities of 0.15, 0.25, 0.35, 0.45, 0.50, and 0.60 V/nm, respectively. For comparison, a MD simulation in the absence of an external electric field was also carried out for 1 μs. All the electric fields were applied in the same arbitrary direction, i.e., along the *X*-axis of the equilibrated system. In addition, some shorter MD runs were performed under higher external electric fields, because conformational changes of the protein occur in several nanoseconds under those high electric fields.

3. RESULTS AND DISCUSSION

3.1. Applied Electric Field under 0.6 V/nm. *Secondary Structure Analysis.* Previous MD studies demonstrated that only the external electric fields stronger than 0.50 V/nm can induce significant structure changes, whereas the lower electric field strength around 0.1 V/nm does not alter the overall structure of the protein within 100 ns MD simulations. In this study, we investigate long-time effects on insulin's secondary structure under a series of electric fields ranging from 0.15 to 0.6 V/nm during 1 μs MD simulation. We initially performed MD simulation with the Amber99SB[56] force field and TIP3P water model. However, this force field did not maintain the overall secondary structure of the bovine insulin in our MD simulation even in the absence of an external electric field. Because this protein is mainly composed of α-helical structures, it has been shown that the Amber03 force field gives a more stable description of intramolecular interaction for helical protein structures.[57,58] Therefore, the Amber03 force field and TIP3P water model were adopted for the protein and solvent, respectively, in all MD simulations.

The evolutions of protein secondary structure as a function of simulation time under different external electric fields ranging from 0 to 0.60 V/nm were plotted in Figure 1a–g. As shown in Figure 1g, under the external electric field of 0.60 V/nm, part of the α-helix (residues 2–6, colored in blue) started to change into the turn structure (colored in yellow) in about 10 ns. This part of the α-helical structure was destroyed and turned into the coil structure completely in around 150 ns (marked with the red border in Figure 1g). For comparison, this helical structure remained stable during 500–1000 ns in the absence of an external electric field (Figure 1a). Moreover, the time evolution of the secondary structure for chain-B (residues 22 to 51) under 0.6 V/nm (Figure 1g) is quite different from that in the absence of an external electric field (Figure 1a). In particular, the section (residues 38–42) centered at residue 40 in both Figure 1g (highlighted with the red brace) and Figure 1a changed into something between turn (colored in yellow) and α-helical (colored in blue) structures during MD simulation. Nevertheless, it tends to be more helical in the absence of the electric field than in the electric field of 0.6 V/nm. On the contrary, the section (residues 17–21) centered at residue 19 (highlighted with the red brace) became more helical in the electric field of 0.6 V/nm than in the absence of an electric field. Furthermore, the section (residues 29–33) centered at residue 31 changed into a turn structure from the α-helix under 0.6 V/nm external electric field in about 210 ns and it further turned into a bend structure (colored in green) in about 360 ns (marked with the red border). For comparison, this section of the protein was always in the α-helical form in the absence of the electric field. A previous study[18] on pig insulin by Budi et al. has demonstrated that the presence of chain-A affected the stability of chain-B in

dx.doi.org/10.1021/jp501051r | J. Phys. Chem. A XXXX, XXX, XXX–XXX

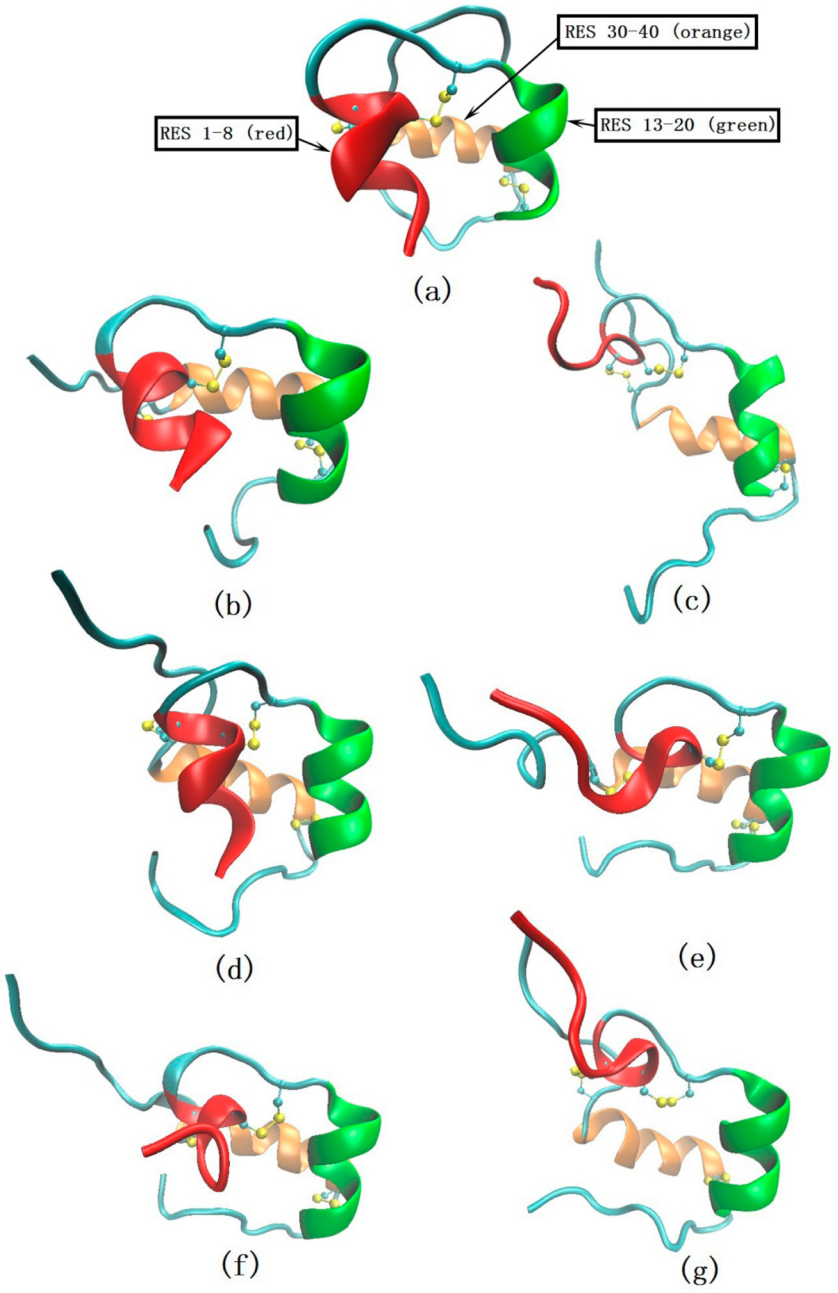

Figure 2. Representative three-dimensional protein structures of the bovine insulin. The disulfide bond is represented by balls and sticks. The structures without external electric field (a) and in the external electric field of 0.15 V/nm (b) are the final structure from 1 μs MD simulations. The other structures in external electric fields of 0.25 (c), 0.35 (d), 0.45 (e), 0.50 (f), and 0.60 V/nm (g) are taken from the snapshots when the secondary structures have just had dramatic changes.

external electric fields by changing the total dipole moment of the protein and lowered the threshold value of the electric field that can cause the disruption of the secondary structure from 1.0 to 0.5 V/nm. Nevertheless, our study shows that the secondary structure of chain-B was not obviously destroyed under the external electric field of 0.6 V/nm in 10 ns, which is within the MD simulation time frame in Budi et al.'s study.[18] The disagreement may come from the difference of the force fields used in MD simulations. As mentioned above, we adopted the Amber03 force field in this study, whereas the MD simulation carried out by Budi et al. used the Charmm27 force field.

A series of MD simulations which are up to 1 μs in external electric fields of 0.50, 0.45, 0.35, 0.25, and 0.15 V/nm, were carried out to probe the threshold value of the electric field, which could cause the disruption of the secondary structure of the protein. The total dipole moment of the protein aligns with the direction of the external electric field quickly (within 1 ns) under the action of those electric fields (Figure S1 of the Supporting Information). As shown in Figure 1, the secondary structure of residues 2−6 was destroyed (from the helical structure to coil structure) under the action of 0.25, 0.45, and 0.50 V/nm (Figure 1c,e,f, respectively) external electric fields during 1 μs MD simulation, whereas this section kept the helical structure in the action of 0.15 and 0.35 V/nm (Figure

dx.doi.org/10.1021/jp501051r | J. Phys. Chem. A XXXX, XXX, XXX−XXX

1b,d) external electric fields. Therefore, the time when this helical region began to be disrupted is not directly correlated with the intensity of the external electric field when its strength ranges from 0.15 to 0.60 V/nm. For comparison, the representative secondary structures of the bovine insulin under different external electric fields ranging from 0 to 0.60 V/nm are shown in Figure 2a−g. One of the helices (residues 13−20) of the protein was placed in the parallel direction for all the structures. One can see from Figure 2 that the red helical section (residues 1−8) was disrupted in the action of 0.25, 0.45, 0.50, and 0.60 V/nm (Figure 2c,e−g, respectively) comparing with that in the absence of an external electric field (Figure 2a). There is no dramatic change in the secondary structure of this section in the action of 0.15 and 0.35 V/nm (Figure 2b,d) from that in the absence of an external electric field. However, a significant difference exists for the section (residues 22−29) centered at the residue 25 between in the presence and in the absence of an external electric field, which is mainly because the external electric field has a significant effect on the dynamical behavior of the loop region of the protein. Similar to the difference of time evolution of the secondary structure between under the 0.60 V/nm electric field and in the absence of an electric field for the section (residues 17−21) centered at residue 19, this region shows more α-helical feature than the turn structure in the action of 0.35, 0.45, and 0.50 V/nm (Figure 1d−f) external electric fields, as compared to the case in the absence of an electric field (Figure 1a) during MD simulation. However, this section shows more 3^{10} helical feature (colored in gray) under external electric fields of 0.15 and 0.25 V/nm (Figure 1b,c). Furthermore, for the section (residues 38−42) centered at residue 40, it shows more turn structure under the action of 0.15, 0.25, 0.35, 0.45, and 0.50 V/nm electric fields than in the absence of an electric field, which is similar to the case in the action of 0.60 V/nm electric field. The secondary structure of the section (residues 6−9) centered at residue 7 shows the turn structure during the whole 1 μs MD simulation in the absence of the external electric field. In contrast, the secondary structure of this section becomes the α-helix occasionally under external electric fields of 0.15 and 0.25 V/nm (Figure 1b,c) during 1 μs MD simulation, whereas this section mostly becomes the α-helix under external electric fields of 0.45 and 0.60 V/nm, as shown in Figure 1e,g, respectively.

Effect on Hydrogen Bonds. It was found that the secondary structure of the bovine insulin was destroyed under the action of the 0.25 V/nm or higher electric field. However, the time evolution of the secondary structure under the external electric field of 0.15 V/nm also shows a clear difference in comparison to that without the external electric field. Herein, we investigate the effect of electric field on the hydrogen bond length. In this study, we define the distance between the main-chain nitrogen atom and oxygen atom as the hydrogen bond length. Figure 3 shows the hydrogen bond (between residues 5 and 9) length distribution in the absence of an electric field and under external electric fields of 0.25 and 0.60 V/nm, respectively. As can be seen from Figure 3, the hydrogen bond length at the peak position of its distribution became shorter in the presence of external electric fields. Because the hydrogen bonds are closely associated with the secondary structure of this subunit (residues 5−9) centered at residue 7, the secondary structure transferred into the α-helix from the turn structure under the external electric fields, as discussed in the previous section. There are two disulfide bonds in this subunit, one is formed between residues 6 and 11 in chain-A and the other one is

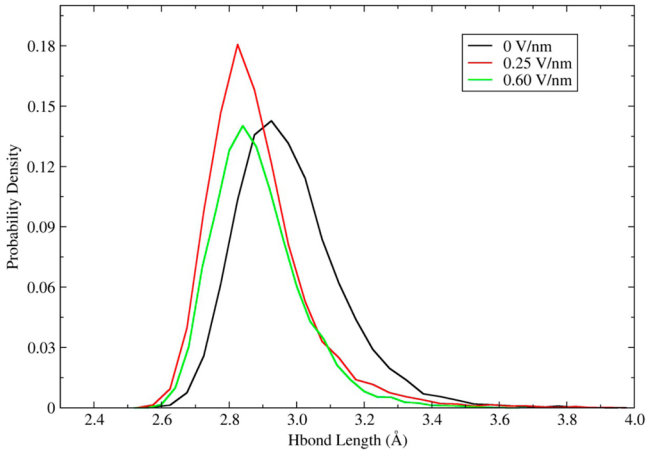

Figure 3. Comparison of the hydrogen bond (between residues 5 and 9) length distributions in the absence of the electric field and in the presence of electric fields of 0.25 and 0.60 V/nm, respectively.

formed between residue 7 of chain-A and residue 7 of chain-B. The two disulfide bonds make this subunit very difficult to stretch. When the secondary structure of residues 2−6 transferred from the α-helix into the coil structure, the dipole moment of this part tended to point to the direction of the external electric field, causing the segment of residues 2−6 to drift away from the disulfide bond between residues 6 and 11, which resulted in compressing the hydrogen bond length between residues 5 and 9.

From the secondary structure analysis, we have shown that the applied external electric field makes significant changes on the helical region centered at residue 4 for bovine insulin. The α-helical structure of this section would disappear completely under high electric fields. To further investigate the effect of the external electric field on the protein, we plot the time evolution of the hydrogen bond length between residues 2 and 6 under different external electric fields in Figure 4. In general, when the hydrogen bond length is more than 3.5 Å, the hydrogen bond is disrupted. As shown in Figure 4, the hydrogen bond length is less than 3.5 Å in the absence of an electric field. On the contrary, the hydrogen bond would be disrupted and its length was stretched to more than 9 Å under external electric fields of 0.25, 0.45, 0.50, and 0.60 V/nm, which indicates that this α-helical region becomes almost flat under the action of sufficiently high electric field. There are only small perturbations on this hydrogen bond under the action of the 0.15 V/nm electric field. However, there is no clear correlation between the intensity of applied electric field and the time when the hydrogen bond began to be disrupted. For example, the hydrogen bond was stable during 1 μs MD simulation under the 0.35 V/nm electric field. This implies that the damage on the hydrogen bond by the electric field is still a random event when the applied electric field is less than 0.60 V/nm. Longer MD simulation may be desired to further investigate the dynamic behavior of the bovine insulin under the 0.35 V/nm electric field.

Figure 5 shows the evolution of the number of hydrogen bonds between the insulin and water molecules as a function of MD simulation time under various external electric fields. One can see from the figure that the number of hydrogen bonds increased significantly under the action of the 0.60 V/nm external electric field as compared to the case in the absence of an external electric field. The number of hydrogen bonds also

dx.doi.org/10.1021/jp501051r | J. Phys. Chem. A XXXX, XXX, XXX−XXX

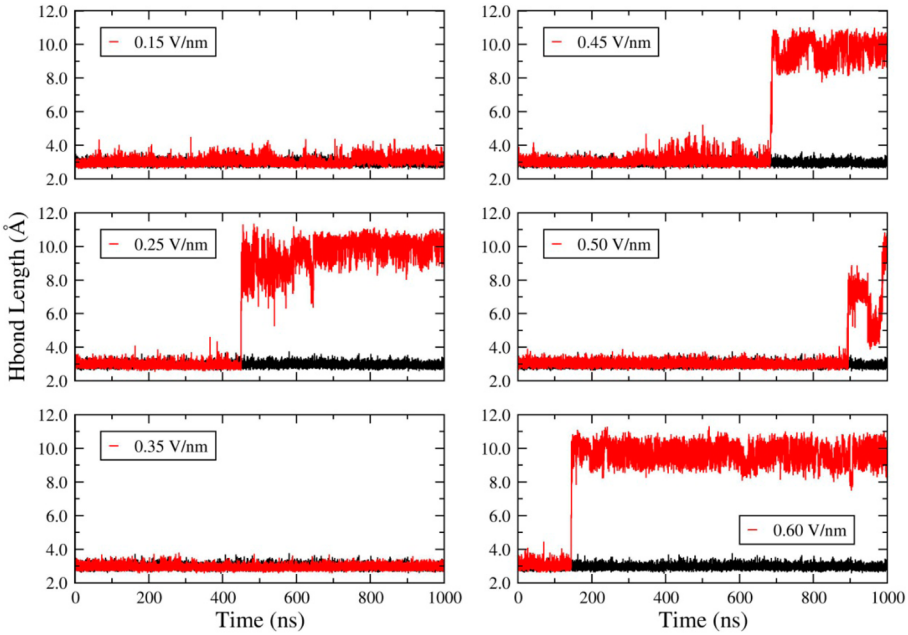

Figure 4. Hydrogen bond length between residues 2 and 6 as a function of simulation time. The black line shows the result in the absence of the external electric field (as the reference), whereas the red lines denote the results for different external electric fields.

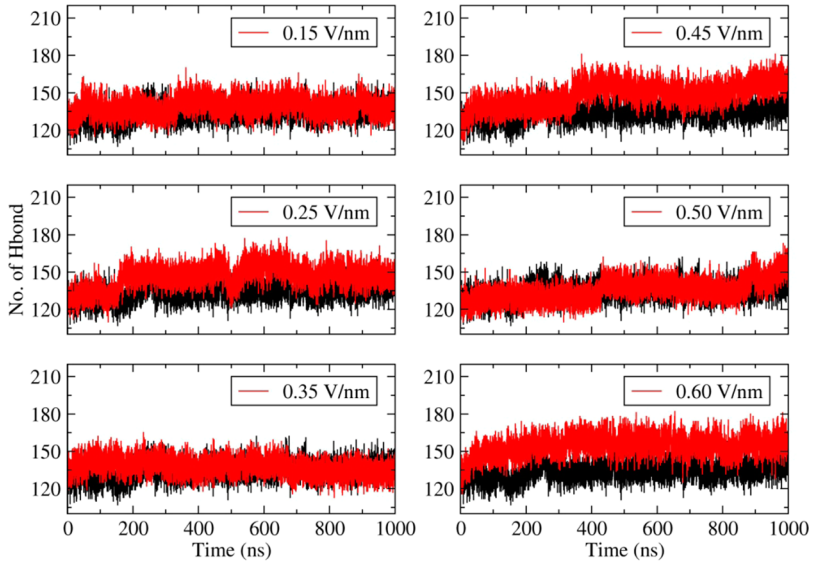

Figure 5. Number of hydrogen bonds (Hbond) between the insulin and water molecules as a function of the MD simulation time. The black line represents the result in the absence of the external electric field (as the reference), whereas the red lines denote the results under various external electric fields.

increased slightly under lower electric fields (0.25, 0.45, and 0.50 V/nm). Because the secondary structure of insulin was stretched under those electric fields, the residues which previously interacted with other parts of the protein were now more accessible by the solvent, resulting in the number of hydrogen bonds between the protein and water molecules increasing accordingly.

RMSD Analysis and Dipole Moment. The external electric field had different effects on the evolution of the α-helical region of residues 1−6 and its neighboring section (residues 7−10). To investigate the stability of these two parts in the external electric fields, we plotted the backbone RMSDs of residues 1−6 and residues 7−10 under different external electric fields in Figure 6. The RMSD is calculated with respect to the starting geometry of 1 μs MD simulation. As can be seen from Figure 6, the RMSD of residues 1−6 increases significantly under external electric fields of 0.25, 0.45, 0.50, and 0.60 V/nm, which shows a remarkable change in the secondary structure of this helical region, whereas the RMSD of residues 7−10 is quite stable under different electric fields.

Figure 7 shows the total dipole moment of the bovine insulin as a function of simulation time in different electric fields. The total dipole moment in the presence of electric fields grows larger than that in the absence of an external electric field. The total dipole moment of the protein is not stable in 1 μs MD simulation under external electric fields of 0.25, 0.45, 0.50, and 0.60 V/nm, which indicates that the influence of electric field on the total dipole moment of protein is a cumulative effect

dx.doi.org/10.1021/jp501051r | J. Phys. Chem. A XXXX, XXX, XXX−XXX

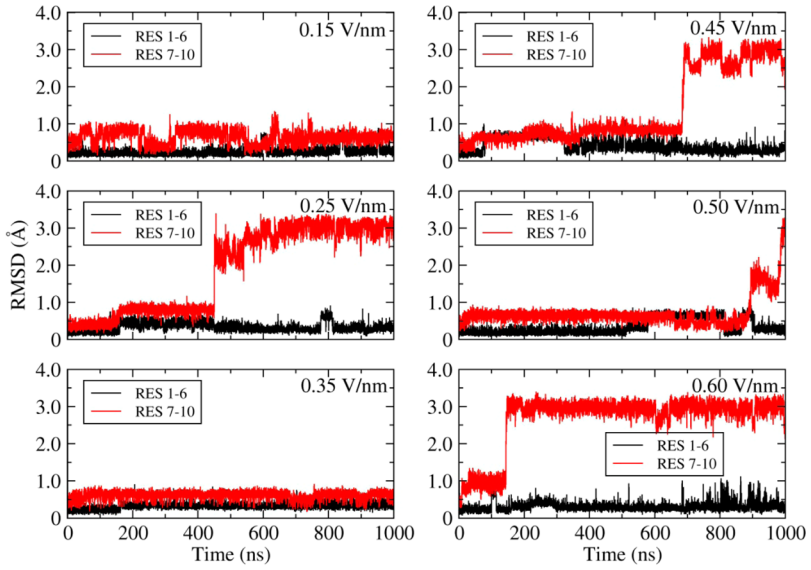

Figure 6. Comparison of backbone RMSDs for residues 1−6 and residues 7−10 of the bovine insulin in the presence of different external electric fields.

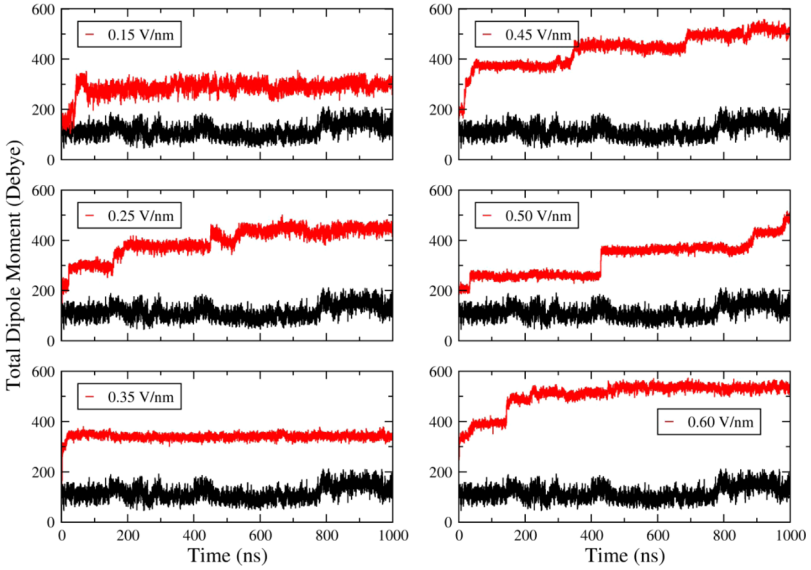

Figure 7. Total dipole moment of the bovine insulin as a function of MD simulation time. The data refer to the results in the absence (black line) and in the presence (red line) of different external electric fields.

over time. The gradual change of the total dipole moment was related to the polarization effect on the protein induced by the external electric field, whereas those dramatic changes were corresponding to denaturation of the protein secondary structure. As shown in Figure 7, some dramatic changes of the total dipole moment happen after 400 ns MD simulation under electric fields of 0.25, 0.45, and 0.50 V/nm. Therefore, we conclude that long time MD simulation (longer than 400 ns) is necessary for investigating the effect of external electric field on proteins for the electric field below 0.6 V/nm.

3.2. Applied Electric Fields above 0.6 V/nm. Figure 8 shows the time evolution of the two hydrogen bonds between residues 2 and 6, residues 13 and 17 under external electric fields of 0.50, 0.60, 0.70, 0.90, and 1.00 V/nm, respectively. The lifetime of the hydrogen bond between residues 2 and 6 is less than 10 ns in external electric fields of 0.90 and 1.00 V/nm. In contrast, more than 150 ns MD simulation is needed to investigate the stability of this hydrogen bond if the applied external electric field is less than or equal to 0.60 V/nm. The hydrogen bond was not disrupted in 120 ns MD simulation under 0.70 V/nm electric field, whereas the other hydrogen bond between residues 13 and 17 was broken in 10 ns under 0.70 V/nm. Although the hydrogen bond between residues 13 and 17 was not completely disrupted under external electric fields of 0.50 and 0.60 V/nm, the fluctuation of this hydrogen bond length is more notable under 0.50 and 0.60 V/nm than in the absence of an external electric field. Both of the hydrogen bonds were broken in about 5 ns under 0.90 and 1.00 V/nm. Only when the external electric field is higher than or equal to 0.90 V/nm were these two hydrogen bonds disrupted in short MD simulations (within 10 ns).

Figure 9 shows the backbone RMSDs of three α-helices with respect to those in the starting structure of the bovine insulin. The obvious changes of the RMSDs mostly happened in 10 ns

dx.doi.org/10.1021/jp501051r | J. Phys. Chem. A XXXX, XXX, XXX−XXX

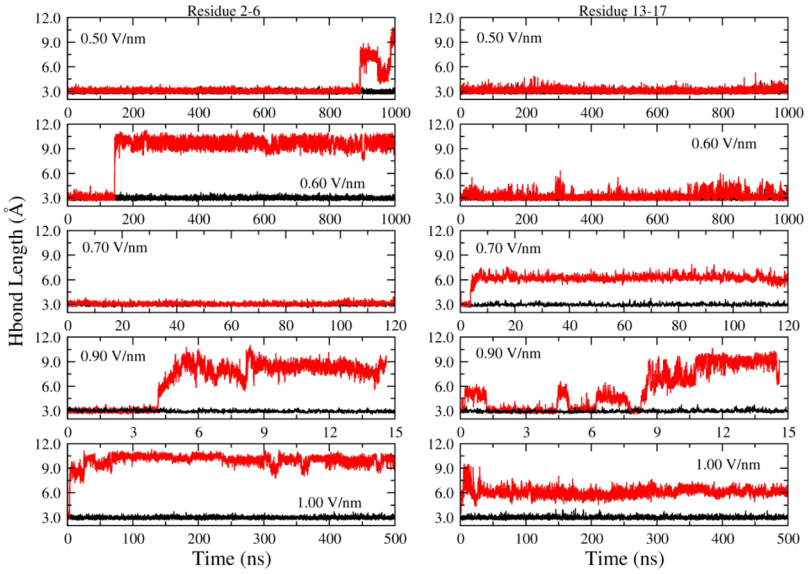

Figure 8. Comparison of hydrogen bond length in the presence of different external electric fields (red line) and without the external electric field (black line) for two typical hydrogen bonds. One hydrogen bond (left column) is between the main chain atoms of residues 2 and 6, and the other one (right column) is between the main chain atoms of residues 13 and 17.

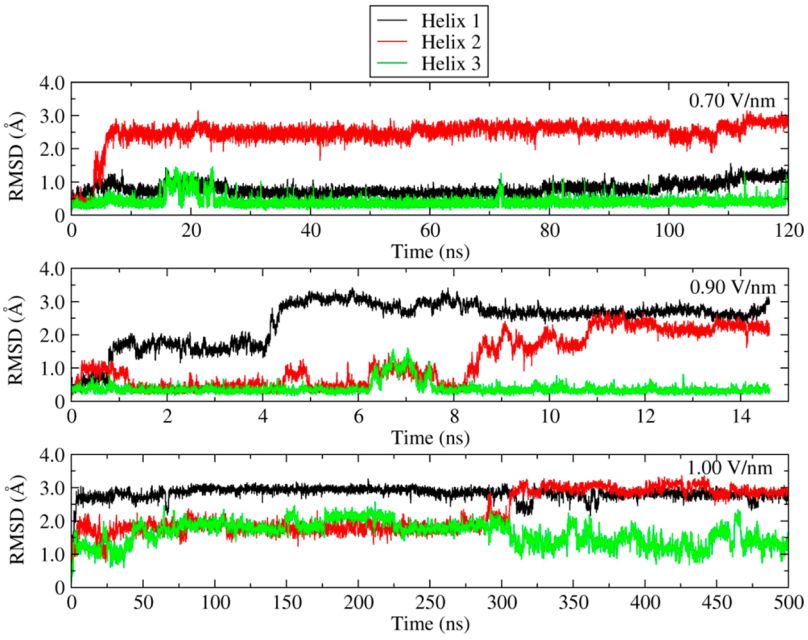

Figure 9. Comparison of RMSDs of different helical regions in the bovine insulin under external electric fields of 0.70, 0.90, and 1.00 V/nm. Helices 1, 2, and 3 represent residues 1−8, 13−20, and 30−40, respectively.

under electric fields of 0.70, 0.90, and 1.0 V/nm. These RMSD changes were closely related to the damage of protein secondary structure and the destruction of hydrogen bonds. As shown in Figure 9, helix 2 (residues 13−20) is more vulnerable to electric fields than helix 1 (residues 1−8) and helix 3 (residues 30−40) under 0.70 V/nm. However, the fluctuation of helix 1 is most significant under 0.90 V/nm. The RMSDs of these three helices all went up in very short time under 1.0 V/nm, which reveals that the 1.0 V/nm electric field would destroy the secondary structure of the protein very rapidly.

Figure 10a shows the time evolution of the protein secondary structure both in the absence of an external electric field and in the presence of the 1.0 V/nm electric field. As shown in the right panel of Figure 10a, the proportion of blue color was reduced as soon as the external electric field of 1.0 V/nm switched on, indicating that the proportion of α-helix in the protein decreased dramatically. In particular, the region from residues 15−20 interchanged between the turn structure and α-helix in the first 300 ns and the α-helical structure disappeared completely after 300 ns. Moreover, the α-helical region centered at residue 4 (shown in the absence of an external electric field) was transformed to the random coil structure in the whole MD simulation under the external electric field of 1.0 V/nm. The neighboring region centered at residue 7, which was shown as the turn structure in the absence of an external electric field, sometimes became the α-helix in the 1.0 V/nm electric field.

dx.doi.org/10.1021/jp501051r | J. Phys. Chem. A XXXX, XXX, XXX−XXX

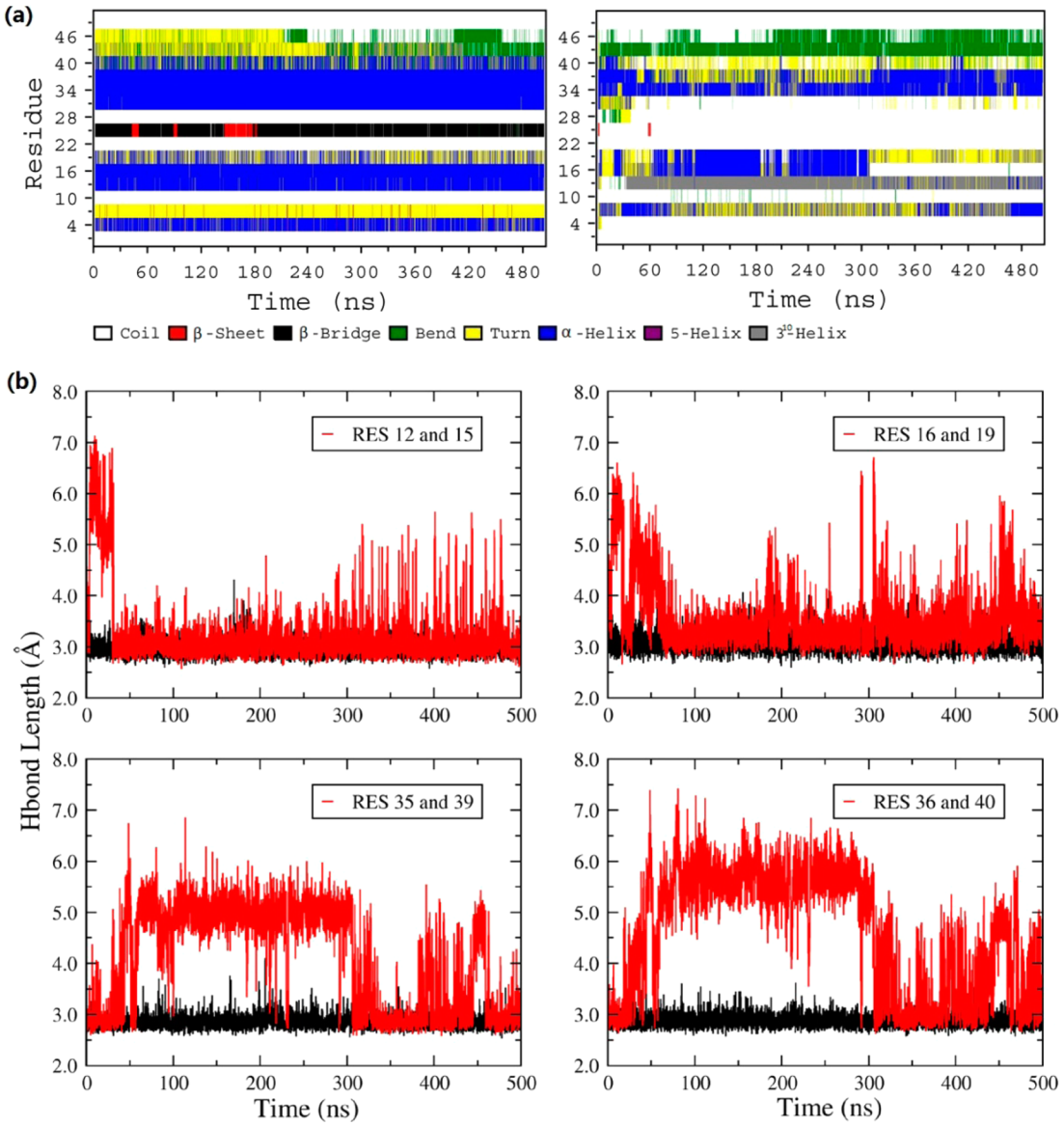

Figure 10. (a) Time evolution of the secondary structure of the bovine insulin in the absence (left) and in the presence of the 1.0 V/nm electric field (right). (b) Comparison of the hydrogen bond length under the 1.0 V/nm electric field (red line) and without the external electric field (black line) for four hydrogen bonds.

Most hydrogen bonds were disrupted in the 1.0 V/nm electric field in less than 10 ns. It is worth noting that the two hydrogen bonds between residues 12 and 15 and between 16 and 19 were broken in less than 1 ns (hydrogen bond length is more than 6.0 Å, see Figure 10b), but these two hydrogen bonds formed again after 30 ns MD simulation (hydrogen bond length is less than 3.5 Å). These two hydrogen bonds are associated with two α-helical regions centered at residue 13 and at residue 17, respectively. As shown in the right panel of Figure 10a, these two regions show a more complicated evolution pattern in color. As for the other two hydrogen bonds between residues 35 and 39 and between residues 36 and 40, they were broken at around 30 ns, and then both tended to form the hydrogen bonds again after 300 ns. The two regions associated with these two hydrogen bonds interchanged between the turn structure and α-helix during the time evolution of the secondary structure. The rapid evolution (forming and breaking) of the four hydrogen bonds in the high electric field demonstrates that different microwaves could either faciliate protein folding or destroy the secondary structure of globular proteins deponding on the intensity of the external electric field.[3]

4. CONCLUSION

Our MD simulation shows that there is a threshold value of the external electric field that could destroy the secondary structure of proteins. This threshold value for the bovine insulin is between 0.15 and 0.25 V/nm. The extent of damage on different domains of insulin in the external electric field is different. The α-helical region (residues 1−6) centered at residue 4 is the easiest to destroy, whereas its neighboring helical section of residues 7−10 is relatively stable due to the disulfide bond between residues 6 and 11. Although the external electric field that could disrupt the helical section of residues 1−6 did not obviously destroy the secondary structure of other domains of insulin, the time evolution of the secondary structure for those domains is quite different from that without the external electric field. In addition, longer MD simulation

dx.doi.org/10.1021/jp501051r | J. Phys. Chem. A XXXX, XXX, XXX−XXX

(more than 1 μs) may be also needed to further investigate the dynamical behavior for those domains of the bovine insulin under the external electric field of 0.35 V/nm.

Although the external electric field between 0.25 and 0.60 V/nm can disrupt the secondary structure of the bovine insulin, the variation of the total dipole moment of insulin during MD simulation shows that the cumulative effect over long simulation time is the major cause of the damage on the secondary structure of insulin. The time when the helical region began to be disrupted is not clearly correlated with the intensity of the external electric field when its strength ranges from 0.15 to 0.60 V/nm, which indicates that there is still some randomness for the damage on the secondary structure in this range of the electric field. When the external electric field is higher than 0.70 V/nm, the damage of the secondary structure of insulin would happen in a very short time.

The time evolution of some key hydrogen bond lengths demonstrates that the damage of the secondary structure under the external electric field stems from the breakdown of corresponding hydrogen bonds. In addition, the hydrogen bonds were disrupted in short MD simulations when the applied external electric field is higher than 0.70 V/nm. The fast evolution (forming and breaking) of some hydrogen bonds of the bovine insulin under 1.0 V/nm electric field implies that different microwaves could either speed up protein folding or destroy the secondary structure of globular proteins depending on the intensity of the applied electric field.

■ ASSOCIATED CONTENT

Supporting Information

Figure S1 gives the angle between the total dipole moment of insulin and the applied external electric field as a function of time in the absence and in the presence of various external electric fields. This material is available free of charge via the Internet at http://pubs.acs.org.

■ AUTHOR INFORMATION

Corresponding Authors

*X. He: e-mail: xiaohe@phy.ecnu.edu.cn.

*J. Z. H. Zhang: e-mail, zhzhang@phy.ecnu.edu.cn.

Notes

The authors declare no competing financial interest.

■ ACKNOWLEDGMENTS

This work was supported by the National Natural Science Foundation of China (Grants No. 20933002 and 21303057) and Shanghai PuJiang program (09PJ1404000). X.H. is also supported by the Specialized Research Fund for the Doctoral Program of Higher Education (Grant No. 20130076120019) and the Fundamental Research Funds for the Central Universities. We thank the Supercomputer Center of East China Normal University for providing us computational time.

■ REFERENCES

(1) de Pomerai, D. I.; Smith, B.; Dawe, A.; North, K.; Smith, T.; Archer, D. B.; Duce, I. R.; Jones, D.; Candido, P. M. Microwave Radiation Can Alter Protein Conformation without Bulk Heating. *FEBS Lett.* **2003**, *543*, 93−97.

(2) Breton, M.; Delemotte, L.; Silve, A.; Mir, L. M.; Tarek, M. Transport of Sirna through Lipid Membranes Driven by Nanosecond Electric Pulses: An Experimental and Computational Study. *J. Am. Chem. Soc.* **2012**, *134*, 13938−13941.

(3) Bohr, H.; Bohr, J. Microwave-Enhanced Folding and Denaturation of Globular Proteins. *Phys. Rev. E* **2000**, *61*, 4310−4314.

(4) Budi, A.; Legge, F. S.; Treutlein, H.; Yarovsky, I. Electric Field Effects on Insulin Chain-B Conformation. *J. Phys. Chem. B* **2005**, *109*, 22641−22648.

(5) English, N. J.; Mooney, D. A. Denaturation of Hen Egg White Lysozyme in Electromagnetic Fields: A Molecular Dynamics Study. *J. Chem. Phys.* **2007**, *126*, 091105.

(6) Astrakas, L.; Gousias, C.; Tzaphlidou, M. Electric Field Effects on Chignolin Conformation. *J. Appl. Phys.* **2011**, *109*, 094702.

(7) Toschi, F.; Lugli, F.; Biscarini, F.; Zerbetto, F. Effects of Electric Field Stress on a β–Amyloid Peptide. *J. Phys. Chem. B* **2009**, *113*, 369−376.

(8) Marracino, P.; Apollonio, F.; Liberti, M.; d'Inzeo, G.; Amadei, A. Effect of High Exogenous Electric Pulses on Protein Conformation: Myoglobin as a Case Study. *J. Phys. Chem. B* **2013**, *117*, 2273−2279.

(9) Baldwin, R. L. Temperature Dependence of the Hydrophobic Interaction in Protein Folding. *Proc. Natl. Acad. Sci. U. S. A.* **1986**, *83*, 8069−8072.

(10) Day, R.; Bennion, B. J.; Ham, S.; Daggett, V. Increasing Temperature Accelerates Protein Unfolding without Changing the Pathway of Unfolding. *J. Mol. Biol.* **2002**, *322*, 189−203.

(11) Hawley, S. A. Reversible Pressure-Temperature Denaturation of Chymotrypsinogen. *Biochemistry* **1971**, *10*, 2436−2442.

(12) Wiedersich, J.; Kohler, S.; Skerra, A.; Friedrich, J. Temperature and Pressure Dependence of Protein Stability: The Engineered Fluorescein-Binding Lipocalin Flua Shows an Elliptic Phase Diagram. *Proc. Natl. Acad. Sci. U. S. A.* **2008**, *105*, 5756−5761.

(13) Panick, G.; Malessa, R.; Winter, R.; Rapp, G.; Frye, K. J.; Royer, C. A. Structural Characterization of the Pressure-Denatured State and Unfolding/Refolding Kinetics of Staphylococcal Nuclease by Synchrotron Small-Angle X-Ray Scattering and Fourier-Transform Infrared Spectroscopy. *J. Mol. Biol.* **1998**, *275*, 389−402.

(14) Shen, L. L.; Hermans, J., Jr. Kinetics of Conformation Change of Sperm-Whale Myoglobin. I. Folding and Unfolding of Metmyoglobin following pH Jump. *Biochemistry* **1972**, *11*, 1836−1841.

(15) Jones, C. M.; Henry, E. R.; Hu, Y.; Chan, C. K.; Luck, S. D.; Bhuyan, A.; Roder, H.; Hofrichter, J.; Eaton, W. A. Fast Events in Protein Folding Initiated by Nanosecond Laser Photolysis. *Proc. Natl. Acad. Sci. U. S. A.* **1993**, *90*, 11860−11864.

(16) Budi, A.; Legge, F. S.; Treutlein, H.; Yarovsky, I. Effect of Frequency on Insulin Response to Electric Field Stress. *J. Phys. Chem. B* **2007**, *111*, 5748−5756.

(17) Zhao, W.; Yang, R. J. Experimental Study on Conformational Changes of Lysozyme in Solution Induced by Pulsed Electric Field and Thermal Stresses. *J. Phys. Chem. B* **2010**, *114*, 503−510.

(18) Budi, A.; Legge, F. S.; Treutlein, H.; Yarovsky, I. Comparative Study of Insulin Chain-B in Isolated and Monomeric Environments under External Stress. *J. Phys. Chem. B* **2008**, *112*, 7916−7924.

(19) Zhao, W.; Yang, R. J. Effect of High-Intensity Pulsed Electric Fields on the Activity, Conformation and Self-Aggregation of Pepsin. *Food Chem.* **2009**, *114*, 777−781.

(20) Sakurai, T.; Terashima, S.; Miyakoshi, J. Effects of Strong Static Magnetic Fields Used in Magnetic Resonance Imaging on Insulin-Secreting Cells. *Bioelectromagnetics* **2009**, *30*, 1−8.

(21) Chen, T.; Lin, S. L.; Lin, J. P.; Zhang, L. S. Effect of Electrical Field on Polypeptide Phase Behavior Involving a Conformationally Coupled Anisotropic-Isotropic Transition. *Polymer* **2007**, *48*, 2056−2063.

(22) Zhao, W.; Yang, R. J. Protective Effect of Sorbitol on Enzymes Exposed to Microsecond Pulsed Electric Field. *J. Phys. Chem. B* **2008**, *112*, 14018−14025.

(23) Chen, Y. B.; Li, J.; Qi, Y. H.; Miao, X.; Zhou, Y. C.; Ren, D. Q.; Guo, G. Z. The Effects of Electromagnetic Pulses (EMP) on the Bioactivity of Insulin and a Preliminary Study of Mechanism. *Int. J. Radiat. Biol.* **2010**, *86*, 22−26.

(24) Lugli, F.; Toschi, F.; Biscarini, F.; Zerbetto, F. Electric Field Effects on Short Fibrils of Aβ Amyloid Peptides. *J. Chem. Theory Comput.* **2010**, *6*, 3516−3526.

(25) Solomentsev, G. Y.; English, N. J.; Mooney, D. A. Hydrogen Bond Perturbation in Hen Egg White Lysozyme by External Electromagnetic Fields: A Nonequilibrium Molecular Dynamics Study. *J. Chem. Phys.* **2010**, *133*, 235102.
(26) Damm, M.; Nusshold, C.; Cantillo, D.; Rechberger, G. N.; Gruber, K.; Sattler, W.; Kappe, C. O. Can Electromagnetic Fields Influence the Structure and Enzymatic Digest of Proteins? A Critical Evaluation of Microwave-Assisted Proteomics Protocols. *J. Proteomics* **2012**, *75*, 5533−5543.
(27) Xie, Y.; Liao, C. Y.; Zhou, J. Effects of External Electric Fields on Lysozyme Adsorption by Molecular Dynamics Simulations. *Biophys. Chem.* **2013**, *179*, 26−34.
(28) George, D. F.; Bilek, M. M.; McKenzie, D. R. Non-Thermal Effects in the Microwave Induced Unfolding of Proteins Observed by Chaperone Binding. *Bioelectromagnetics* **2008**, *29*, 324−330.
(29) Zhao, W.; Yang, R. J.; Zhang, H. Q. Recent Advances in the Action of Pulsed Electric Fields on Enzymes and Food Component Proteins. *Trends Food Sci. Technol.* **2012**, *27*, 83−96.
(30) Luo, Z. X.; Loo, B. H.; Cao, X. Q.; Peng, A. D.; Yao, J. N. Probing the Conformational Transition of 2,2′-Bipyridyl under External Field by Surface-Enhanced Raman Spectroscopy. *J. Phys. Chem. C* **2012**, *116*, 2884−2890.
(31) Starzyk, A.; Cieplak, M. Proteins in the Electric Field near the Surface of Mica. *J. Chem. Phys.* **2013**, *139*, 045102.
(32) Shaw, D. E.; Maragakis, P.; Lindorff-Larsen, K.; Piana, S.; Dror, R. O.; Eastwood, M. P.; Bank, J. A.; Jumper, J. M.; Salmon, J. K.; Shan, Y. B.; et al. Atomic-Level Characterization of the Structural Dynamics of Proteins. *Science* **2010**, *330*, 341−346.
(33) Klepeis, J. L.; Lindorff-Larsen, K.; Dror, R. O.; Shaw, D. E. Long-Timescale Molecular Dynamics Simulations of Protein Structure and Function. *Curr. Opin. Struct. Biol.* **2009**, *19*, 120−127.
(34) Rosenbaum, D. M.; Zhang, C.; Lyons, J. A.; Holl, R.; Aragao, D.; Arlow, D. H.; Rasmussen, S. G. F.; Choi, H. J.; DeVree, B. T.; Sunahara, R. K.; et al. Structure and Function of an Irreversible Agonist-β(2) Adrenoceptor Complex. *Nature* **2011**, *469*, 236−240.
(35) Suydam, I. T.; Snow, C. D.; Pande, V. S.; Boxer, S. G. Electric Fields at the Active Site of an Enzyme: Direct Comparison of Experiment with Theory. *Science* **2006**, *313*, 200−204.
(36) Xu, L.; Cohen, A. E.; Boxer, S. G. Electrostatic Fields near the Active Site of Human Aldose Reductase: 2. New Inhibitors and Complications Caused by Hydrogen Bonds. *Biochemistry* **2011**, *50*, 8311−8322.
(37) Wang, X. W.; He, X.; Zhang, J. Z. H. Predicting Mutation-Induced Stark Shifts in the Active Site of a Protein with a Polarized Force Field. *J. Phys. Chem. A* **2013**, *117*, 6015−6023.
(38) Sandberg, D. J.; Rudnitskaya, A. N.; Gascon, J. A. QM/MM Prediction of the Stark Shift in the Active Site of a Protein. *J. Chem. Theory Comput.* **2012**, *8*, 2817−2823.
(39) Fried, S. D.; Bagchi, S.; Boxer, S. G. Measuring Electrostatic Fields in Both Hydrogen-Bonding and Non-Hydrogen-Bonding Environments Using Carbonyl Vibrational Probes. *J. Am. Chem. Soc.* **2013**, *135*, 11181−11192.
(40) Warshel, A.; Russell, S. T. Calculations of Electrostatic Interactions in Biological Systems and in Solutions. *Q. Rev. Biophys.* **1984**, *17*, 283−422.
(41) Warshel, A.; Sharma, P. K.; Kato, M.; Xiang, Y.; Liu, H.; Olsson, M. H. Electrostatic Basis for Enzyme Catalysis. *Chem. Rev.* **2006**, *106*, 3210−3235.
(42) Xiang, Y.; Duan, L.; Zhang, J. Z. Protein's Electronic Polarization Contributes Significantly to Its Catalytic Function. *J. Chem. Phys.* **2011**, *134*, 205101.
(43) Shi, Y.; Zhou, Y.; Wang, S.; Zhang, Y. Sirtuin Deacetylation Mechanism and Catalytic Role of the Dynamic Cofactor Binding Loop. *J. Phys. Chem. Lett.* **2013**, *4*, 491−495.
(44) Rooklin, D. W.; Lu, M.; Zhang, Y. Revelation of a Catalytic Calcium-Binding Site Elucidates Unusual Metal Dependence of a Human Apyrase. *J. Am. Chem. Soc.* **2012**, *134*, 15595−15603.
(45) Astrakas, L. G.; Gousias, C.; Tzaphlidou, M. Structural Destabilization of Chignolin under the Influence of Oscillating Electric Fields. *J. Appl. Phys.* **2012**, *111*, 074702.
(46) Van der Spoel, D.; Lindahl, E.; Hess, B.; Groenhof, G.; Mark, A. E.; Berendsen, H. J. C. Gromacs: Fast, Flexible, and Free. *J. Comput. Chem.* **2005**, *26*, 1701−1718.
(47) Duan, Y.; Wu, C.; Chowdhury, S.; Lee, M. C.; Xiong, G. M.; Zhang, W.; Yang, R.; Cieplak, P.; Luo, R.; Lee, T.; et al. A Point-Charge Force Field for Molecular Mechanics Simulations of Proteins Based on Condensed-Phase Quantum Mechanical Calculations. *J. Comput. Chem.* **2003**, *24*, 1999−2012.
(48) Jorgensen, W. L.; Chandrasekhar, J.; Madura, J. D.; Impey, R. W.; Klein, M. L. Comparison of Simple Potential Functions for Simulating Liquid Water. *J. Chem. Phys.* **1983**, *79*, 926−935.
(49) Smith, G. D.; Pangborn, W. A.; Blessing, R. H. The Structure of T-6 Bovine Insulin. *Acta Crystallogr. Sect. D* **2005**, *61*, 1476−1482.
(50) Berendsen, H. J. C.; Postma, J. P. M.; van Gunsteren, W. F.; DiNola, A.; Haak, J. R. Molecular Dynamics with Coupling to an External Bath. *J. Chem. Phys.* **1984**, *81*, 3684−3690.
(51) Parrinello, M.; Rahman, A. Crystal Structure and Pair Potentials: A Molecular-Dynamics Study. *Phys. Rev. Lett.* **1980**, *45*, 1196−1199.
(52) Hess, B.; Bekker, H.; Berendsen, H. J. C.; Fraaije, J. G. E. M. Lincs: A Linear Constraint Solver for Molecular Simulations. *J. Comput. Chem.* **1997**, *18*, 1463−1472.
(53) Darden, T.; York, D.; Pedersen, L. Particle Mesh Ewald: An N. Log(N) Method for Ewald Sums in Large Systems. *J. Chem. Phys.* **1993**, *98*, 10089−10092.
(54) Kabsch, W.; Sander, C. Dictionary of Protein Secondary Structure: Pattern Recognition of Hydrogen-Bonded and Geometrical Features. *Biopolymers* **1983**, *22*, 2577−2637.
(55) Humphrey, W.; Dalke, A.; Schulten, K. Vmd: Visual Molecular Dynamics. *J. Mol. Graphics* **1996**, *14*, 33−38.
(56) Hornak, V.; Abel, R.; Okur, A.; Strockbine, B.; Roitberg, A.; Simmerling, C. Comparison of Multiple Amber Force Fields and Development of Improved Protein Backbone Parameters. *Proteins: Struct. Funct. Bioinform.* **2006**, *65*, 712−725.
(57) Best, R. B.; Buchete, N.-V.; Hummer, G. Are Current Molecular Dynamics Force Fields Too Helical? *Biophys. J.* **2008**, *95*, L7−L9.
(58) Lei, H.; Wu, C.; Liu, H.; Duan, Y. Folding Free-Energy Landscape of Villin Headpiece Subdomain from Molecular Dynamics Simulations. *Proc. Natl. Acad. Sci. U. S. A.* **2007**, *104*, 4925−4930.